

## **Bridging Field and Laboratory Permeabilities of Pervious Pavement Mixtures Using XRCT-Based Numerical Modeling**

Jagadeesh, A.; Ong, G. P.; Su, Y. M.

**DOI**

[10.1061/JMCEE7.MTENG-16311](https://doi.org/10.1061/JMCEE7.MTENG-16311)

**Publication date**

2024

**Document Version**

Final published version

**Published in**

Journal of Materials in Civil Engineering

**Citation (APA)**

Jagadeesh, A., Ong, G. P., & Su, Y. M. (2024). Bridging Field and Laboratory Permeabilities of Pervious Pavement Mixtures Using XRCT-Based Numerical Modeling. *Journal of Materials in Civil Engineering*, 36(4), Article 04024026. <https://doi.org/10.1061/JMCEE7.MTENG-16311>

**Important note**

To cite this publication, please use the final published version (if applicable). Please check the document version above.

**Copyright**

Other than for strictly personal use, it is not permitted to download, forward or distribute the text or part of it, without the consent of the author(s) and/or copyright holder(s), unless the work is under an open content license such as Creative Commons.

**Takedown policy**

Please contact us and provide details if you believe this document breaches copyrights. We will remove access to the work immediately and investigate your claim.

***Green Open Access added to TU Delft Institutional Repository***

***'You share, we take care!' - Taverne project***

**<https://www.openaccess.nl/en/you-share-we-take-care>**

Otherwise as indicated in the copyright section: the publisher is the copyright holder of this work and the author uses the Dutch legislation to make this work public.



# Bridging Field and Laboratory Permeabilities of Pervious Pavement Mixtures Using XRCT-Based Numerical Modeling

A. Jagadeesh, Ph.D.<sup>1</sup>; G. P. Ong, Ph.D., M.ASCE<sup>2</sup>; and Y.-M. Su, Ph.D., Aff.M.ASCE<sup>3</sup>

**Abstract:** Drainage capacity of pervious pavement mixtures is commonly measured using a falling head permeameter at hydraulic heads much higher than expected in the field. Recent advancements in computational fluid dynamics (CFD)– and X-ray computed tomography (XRCT)–based modeling eliminates the laboratory challenges of maintaining lower hydraulic heads. However, improper characterization in digital image processing (DIP) and finite-volume simulations resulted in significant errors in permeability measurements and fluid flow behavior. In addition, past studies have identified non-Darcy fluid flow characteristics in pervious pavement mixtures following the Izbash and Forchheimer laws. This paper attempts to bridge this research gap by comparing the Darcy and non-Darcy permeability parameters at different laboratory and field hydraulic heads using advanced XRCT-based modeling. It was found from the analyses that the use of laboratory hydraulic head could result in significant underestimation of permeability parameters compared with the field hydraulic heads for Darcy and Izbash equations (by up to 73%), and overestimation for Forchheimer equations (by up to 216%). Fluid flow behavior in pervious mixtures was found to be in transition flow regime (neither laminar nor turbulent) at both laboratory and field hydraulic gradients. Overall, this study can help in a better fundamental understanding of the current limitations of laboratory measurements and the need for XRCT-based numerical modeling to bridge field and laboratory permeabilities of pervious pavement mixtures. DOI: [10.1061/JMCEE7.MTENG-16311](https://doi.org/10.1061/JMCEE7.MTENG-16311). © 2024 American Society of Civil Engineers.

**Author keywords:** Pervious pavement; Medical X-ray computed tomography (XRCT); Finite-volume simulations; Non-Darcy permeability; Field hydraulic heads.

## Introduction

The measurement of permeability plays a crucial role in determining the drainage performance of pervious pavements (Fwa et al. 2001; Tan et al. 2000). Accurate evaluation of permeability in the laboratory is essential to avoid significant over- or underestimation of drainage properties, which can impact design parameters, such as pore size, outlet pipes, and drainage systems, as well as the selection of appropriate gradations and thicknesses. These factors directly influence the costs and the intended functionality of the pavement in the field (Fwa et al. 1998; Tan et al. 2004; Chen et al. 2020).

Existing guidance and recommendations regarding permeability in pervious pavements primarily rely on experimental Darcy's permeability [ACI 522R-2010 (ACI 2010); ASTM C1701 (ASTM 2017); Cooley 1999]. These approaches assume a linear relationship between permeability and hydraulic head and consider fluid

flow to be laminar. However, these recommendations often involve laboratory permeability measurements at hydraulic heads much higher than typically encountered in field conditions. For instance, ACI 522R-2010 (ACI 2010) suggests a hydraulic head ranging from 70 to 290 mm, while BS EN 12697-19:2012 (BSI 2012) adopts a 300-mm hydraulic head. It was observed by Tan et al. (1997) that Darcy's fluid flow theory does not apply to pervious pavement materials with aggregates or pore sizes greater than 5 mm. To address the issue of nonlinearity and turbulent flow, Tan et al. introduced the use of pressure transducers and developed a non-Darcy equation for hydraulic heads ranging from 25 to 150 mm. Although this study established the nonlinearity between laboratory hydraulic head and permeability in pervious pavement mixtures, it was limited in deriving the flow regime at hydraulic heads below 25 mm [ASTM C1701 (ASTM 2017)], primarily due to measurement constraints posed by the pressure transducers, as illustrated in Fig. 1. In this regard, the utilization of X-ray computed tomography (XRCT)–based simulations holds promise for overcoming the limitations of permeability measurement in pavements at low or field hydraulic heads.

Previous research studies have examined the application of XRCT-based fluid flow simulations to investigate the permeability characteristics of pervious pavements under field hydraulic heads (Masad et al. 2007; Gruber et al. 2012; Zhang et al. 2018; Chen et al. 2018; Jagadeesh et al. 2019a). A summary of the XRCT-based numerical studies on non-Darcy permeability in pervious pavements can be found in Table 1, while Table 2 compares commonly used Darcy and non-Darcy permeability equations in various XRCT-based simulation studies (Bear 1972).

Masad et al. (2007) was the first to utilize XRCT simulations to analyze open-graded friction course (OGFC) samples under field hydraulic gradients. Their work highlighted the nonlinearity of the

<sup>1</sup>Lecturer, Dept. of Engineering Structures, Faculty of Civil Engineering and Geosciences, Delft Univ. of Technology, Delft 2628CN, Netherlands. Email: [a.jagadeesh@tudelft.nl](mailto:a.jagadeesh@tudelft.nl)

<sup>2</sup>Associate Professor, Dept. of Civil and Environmental Engineering, National Univ. of Singapore, Block E1A, #07-03, 1 Engineering Dr. 2, Singapore 117576 (corresponding author). ORCID: <https://orcid.org/0000-0003-3045-4030>. Email: [ceeongr@nus.edu.sg](mailto:ceeongr@nus.edu.sg)

<sup>3</sup>Assistant Professor, Dept. of Civil Engineering, National Kaohsiung Univ. of Science and Technology, 415, Chien-Kung Rd., Sanmin District, Kaohsiung 80778, Taiwan. Email: [yuminsu@nkust.edu.tw](mailto:yuminsu@nkust.edu.tw)

Note. This manuscript was submitted on January 14, 2023; approved on September 27, 2023; published online on January 24, 2024. Discussion period open until June 24, 2024; separate discussions must be submitted for individual papers. This paper is part of the *Journal of Materials in Civil Engineering*, © ASCE, ISSN 0899-1561.

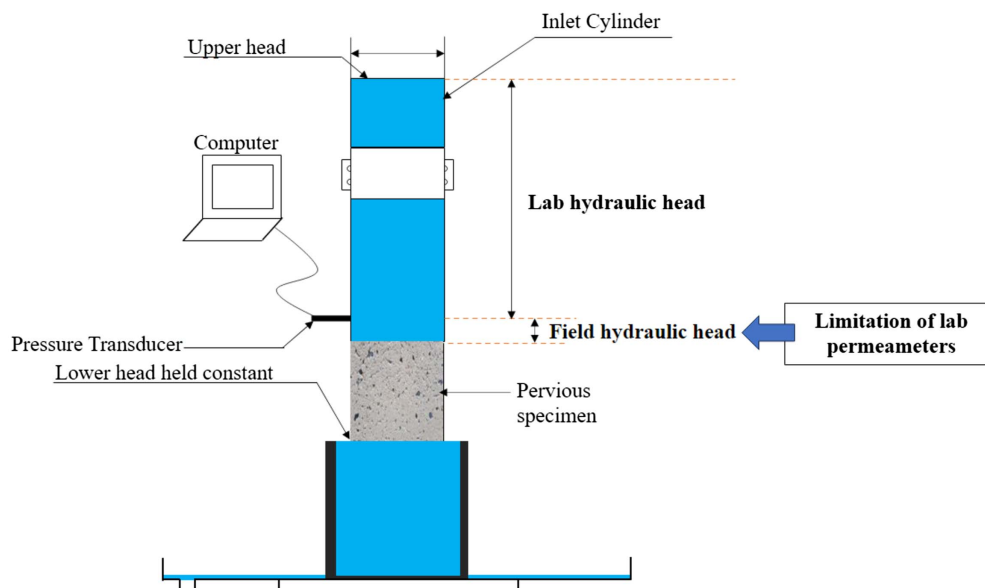


**Fig. 1.** Laboratory falling head permeameter with pressure transducer.

**Table 1.** Literature review on XRCT-based non-Darcy permeability studies and research gap

Reference	Sample	XRCT-based simulations		Advantages	Limitations
		Hydraulic heads	Permeability coefficient		
Masad et al. (2007)	Open-graded friction course	Field	Darcy	<ul style="list-style-type: none"> <li>First study on field nonlinear permeability characteristics using XRCT-based simulations</li> <li>Experimental permeability validation at lab hydraulic heads</li> </ul>	<ul style="list-style-type: none"> <li>Improper DIP algorithms</li> <li>Lack of turbulent modeling</li> <li>Permeability error varies from <math>-100\%</math> to <math>470\%</math></li> <li>Improper flow regime characterization</li> </ul>
Gruber et al. (2012)	Porous asphalt	Lab	Forchheimer	<ul style="list-style-type: none"> <li>Investigated anisotropic permeability, pore size distribution, and Forchheimer coefficients</li> <li>Experimental permeability validation at lab hydraulic heads</li> </ul>	<ul style="list-style-type: none"> <li>Improper DIP algorithms</li> <li>Lack of turbulent modeling</li> <li>Permeability error varies from <math>-60\%</math> to <math>-72\%</math></li> </ul>
Zhang et al. (2018)	Pervious concrete	Field	Darcy and Forchheimer	<ul style="list-style-type: none"> <li>Introduced critical Reynolds number as the boundary of the laminar and turbulent flow</li> <li>Introduced the use of watershed algorithm to divide the single interconnected void structure into multiple voids</li> </ul>	<ul style="list-style-type: none"> <li>Improper DIP algorithms</li> <li>Lack of turbulent modeling</li> <li>Lack of experimental validation</li> <li>Improper flow regime characterization</li> </ul>
Chen et al. (2018)	Porous asphalt	Field	Darcy and Forchheimer	<ul style="list-style-type: none"> <li>Studied the flow regime characterization using Reynolds number</li> </ul>	<ul style="list-style-type: none"> <li>Improper DIP algorithms</li> <li>Lack of watershed algorithm</li> <li>Lack of turbulent modeling</li> <li>Lack of experimental validation</li> <li>Improper flow regime characterization</li> </ul>
Jagadeesh et al. (2019a) and Ong et al. (2020)	Pervious concrete	Lab	Izbash	<ul style="list-style-type: none"> <li>Investigated the effect of thresholding algorithms and pore network properties on permeability</li> <li>Usage of turbulent modeling</li> <li>Experimental permeability validation at lab hydraulic heads</li> </ul>	<ul style="list-style-type: none"> <li>Lack of field permeability characteristics</li> <li>Higher computational time</li> <li>Expensive software</li> </ul>
Current study	Pervious concrete	Lab and field	Darcy and non-Darcy (Forchheimer and Izbash)	<ul style="list-style-type: none"> <li>Proper DIP algorithms</li> <li>Usage of turbulent modeling</li> <li>Experimental permeability validation at lab hydraulic heads</li> <li>Proper flow regime characterization</li> </ul>	<ul style="list-style-type: none"> <li>Higher computational time</li> <li>Expensive software</li> </ul>

**Table 2.** Comparison of Darcy and non-Darcy permeability equations

Permeability equation	Relation between specific discharge $v$ and hydraulic gradient $i$
Darcy	$v = ki$ $k =$ Darcy permeability coefficient
Izbash	$v = ki^m$ $k =$ Izbash permeability coefficient $m =$ flow index
Forchheimer	$i = av + bv^2$ $k = \frac{1}{a}$ $\beta = b \cdot g$ $a, b =$ regression coefficients $k =$ Forchheimer permeability coefficient $\beta =$ Forchheimer coefficient $g =$ acceleration due to gravity (9.81 m/s <sup>2</sup> )

Darcy permeability coefficient with respect to pressure difference. Building on this pioneering research, Zhang et al. (2018), Chen et al. (2018), and Wen et al. (2020) investigated the linear and nonlinear flow characteristics of pervious pavement samples under field hydraulic gradients using parameters such as Reynolds number and various flow equations, including the Darcy and Forchheimer equations. It was noted, however, that these studies by Masad et al. (2007), Gruber et al. (2012), Zhang et al. (2018), Chen et al. (2018), and Wen et al. (2020) did not provide details on the adoption of thresholding, ungrouping, and watershed algorithms. Neglecting proper implementation of digital image processing (DIP) algorithms can lead to significant errors in permeability (Jagadeesh et al. 2019a), pore diameters (Jagadeesh et al. 2020), and Reynolds number, thereby affecting flow regime characterization (laminar, turbulent, or transitional flow). Improper characterization of the flow regime can ultimately result in incorrect adoption of Darcy and non-Darcy equations, leading to further inaccuracies in fluid flow modeling and impacting the drainage performance of pervious pavements. Furthermore, no existing XRCT-based studies in the literature have compared pavement permeability under laboratory and field hydraulic heads.

This paper therefore aims to address this research gap by adopting XRCT scanning, DIP, and finite-volume simulations in the following:

- Developing a numerical model that allows simulation of fluid flow characteristics at field hydraulic gradients,
- Comparing Darcy and non-Darcy (Forchheimer and Izbash) permeability parameters at laboratory and field hydraulic heads, and
- Characterizing fluid flow regime properties using Reynolds number obtained from appropriate DIP algorithms and velocities.

In addressing these objectives, this study provides a novel evaluation of field non-Darcy permeability using accurate XRCT-based simulations by being the first-of-its-kind study to compare the effect of laboratory and field hydraulic heads using XRCT-based simulations. Findings derived in this study can help researchers in quantifying the existing laboratory limitations in measuring the permeabilities and will pave the way for the development of more accurate permeameters or better pavement drainage design.

## Materials and Experiments

In this study, three different pervious concrete mixtures, namely, P1, P2, and P3, were investigated. These mixtures were composed of single-sized and dense-graded aggregates, with the specific compositions detailed in Table 3 [ACI 522R-2010 (ACI 2010); Chandrappa and Biligiri 2016; Jagadeesh et al. 2018; Ong et al. 2020]. The constituent materials and their respective proportions

**Table 3.** Aggregate gradations for various samples considered in study

Mixture	Mass percentage (%) passing the sieve size (mm)				
	19	12.7	9.51	4.76	2.38
P1	100	100	100	0	0
P2	100	100	0	0	0
P3	100	82.6	56	6.3	0

by weight were kept constant throughout the experiment. The materials used in the pervious concrete mixtures included:

- Coarse aggregates: The coarse aggregates were used at a density of 1,530 kg/m<sup>3</sup>.
- Cement: Type I cement [ASTM C150-16E1 (ASTM 2016)] was employed at a density of 340 kg/m<sup>3</sup>.
- Superplasticizer: A superplasticizer was added to enhance the workability of the mixture at a rate of 2 kg/m<sup>3</sup>.
- Water-cement ratio: A water-cement ratio of 0.3 was maintained to ensure the desired consistency and strength.

To create the pervious concrete samples (3 gradations  $\times$  3 replicates, designated as P1-1 to P1-3, P2-1 to P2-3, and P3-1 to P3-3), cylindrical molds with a diameter of 100 mm and height of 180 mm were utilized. Tapping rods were employed during the casting process to achieve proper compaction. Subsequently, the samples were cured in a lime water tank for a duration of 28 days to attain sufficient strength and durability. The laboratory void content, or effective porosity, of the pervious concrete samples was determined using ASTM C1754-12 (ASTM 2012). Drying Method B. For the determination of the non-Darcy permeability coefficient and flow index, a falling head permeameter setup as shown in Fig. 1 was employed. This setup involved applying a falling hydraulic head ranging from 150 to 25 mm upstream while maintaining a constant downstream head. The permeability parameters were obtained through careful measurement and analysis of the flow rates. By employing these materials and experimental procedures in the newly developed XRCT-based models, key limitations in the laboratory measurement of permeability were investigated.

## Methodology

Acknowledging the limitations of laboratory permeability tests in capturing non-Darcy permeability characteristics under field hydraulic heads and the incomplete representation of DIP algorithms and hydraulic gradients in existing XRCT-based permeability studies, this paper introduces an accurate XRCT-scan-based finite-volume permeability simulation model. Fig. 2 illustrates the methodology for determining specific discharge and Reynolds number in pervious pavement mixtures, and this section provides the key steps involved in the process.

### Medical X-Ray Computed Tomography and Image Processing

The Somatom Emotion medical X-ray CT scanner, manufactured by Siemens Healthcare and located in Taiwan, was used to obtain a series of two-dimensional pervious concrete images. The convolution kernel algorithm was used to remove the image noises due to metal artifacts, ring artifacts, and beam hardening. The absorption coefficient of the pixels was converted to 12-bit grayscale values ( $2^{12} = 4,096$ ) varying from 0 to 4,095. The medical CT scanner adopted in this paper enables the accurate measurement of pervious pavement internal structure to within a voxel size of  $0.326 \times 0.326 \times 0.7$  mm. Following are the image preprocessing steps involved:

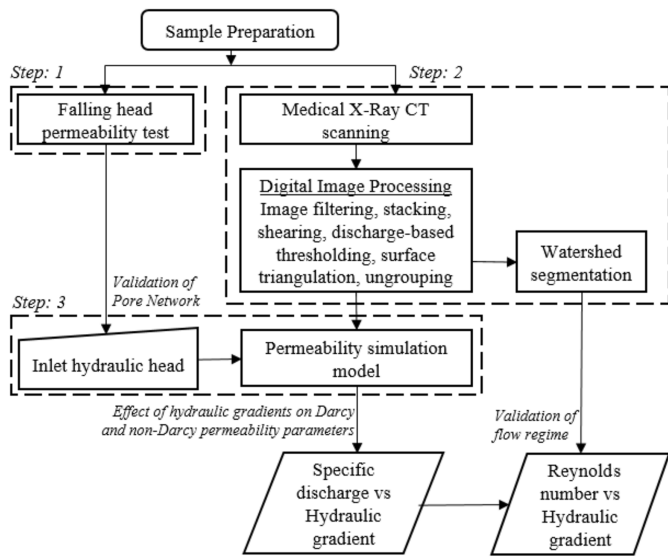


**Fig. 2.** Methodology to compute specific discharge and Reynolds number in pervious concrete.

1. The pixels in a stack of two-dimensional sectional images in the  $XY$ -plane are converted to a grid of three-dimensional voxels by extruding the two-dimensional (2D) images on either side by half the spacing in the  $Z$ -direction such that a three-dimensional (3D) grid of contiguous voxels is formed. The grayscale values of the voxels are then taken directly from their corresponding pixel values in 2D images varying from 0 to 4,095. The image processing software Synopsys Simpleware ScanIP version N-2018.03 was used in this paper to convert the 2D pixel-based CT scan images to 3D voxel-based masks.
2. Image shearing in the  $YZ$ -plane, which is a commonly used prerequisite treatment process for most medical CT scan images due to the difficulty in obtaining a flat surface during the scanning process, is then performed.
3. Image segmentation using a discharge-based thresholding algorithm by Jagadeesh et al. (2019a) is carried out to divide the CT images of varying grayscale intensities into solid and void phases for pervious concrete samples.
4. Surface mask triangulation and meshing using the Enhanced Volumetric Marching Cubes (EVoMaC) algorithm (Young et al. 2008) in Synopsys Simpleware FE module is performed. This meshing algorithm eliminates the drawbacks of voxel-based meshing such as the generation of stepped surface volumetric mesh that can result in an unrealistic LEGO brick appearance and inaccuracies in the permeability simulation and pore parameter results (Young et al. 2008).
5. The ungrouping algorithm is used to remove the isolated pores from the interconnected pore structure. This is followed by the usage of the watershed segmentation algorithm, in which the interconnected pore structure is divided into multiple smaller pores at the geometric constriction points called throats. The watershed segmentation algorithm is mainly used to investigate the average pore network properties of different pervious concrete samples for the determination of Reynolds number.

### Simulation of Fluid Flow in Pervious Pavement Sample

A finite-volume-based permeability simulation model has been developed in the ANSYS CFX 18.1 platform based on the interconnected pore structure reconstructed from Simpleware + ScanFE.

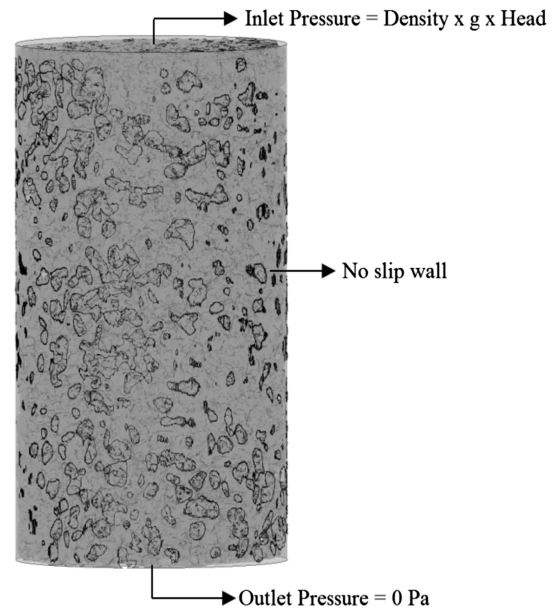


**Fig. 3.** Three-dimensional pervious concrete permeability simulation model.

Fig. 3 shows the three-dimensional volumetric mesh of Sample P1-1 pores along with the applied boundary conditions. The constant pressure boundary conditions are used on top inlet and bottom outlets in the pore structure model. The no-slip wall boundary condition is used on all other surrounding surfaces in the model. Fluid flow behavior in the pore structure is modeled using the Navier-Stokes equations and the  $\hat{k} - \varepsilon$  (turbulent kinetic energy–turbulent eddy dissipation) turbulence equations. The developed XRCT-based computational fluid dynamics (CFD) model can predict the specific discharge  $v$  at various hydraulic heads for pervious concrete samples and the permeability coefficients can be obtained using Table 2. More details on the developed simulation model can be found in Jagadeesh et al. (2019a) and Ong et al. (2020).

The Reynolds number  $Re$  was used in the current study to examine the fluid flow regime characteristics at different hydraulic heads. The dimensionless number  $Re$  was calculated as follows (Tan et al. 1997; Bear 1972):

$$Re = \frac{vd}{\mu_k} \quad (1)$$

where  $v$  = specific discharge or seepage velocity;  $d$  = mean effective pore diameter; and  $\mu_k$  = fluid kinematic viscosity. Based on the

**Table 4.** Experimental validation for effective porosity

Mixture	Sample	Experiment-based effective porosity (%)	XRCT-based effective porosity (%)	Percent Error	Percent error
P1	P1-1	19.45	23.27	3.82	19.66
	P1-2	18.89	23.59	4.70	24.89
	P1-3	18.01	21.18	3.17	17.59
P2	P2-1	19.66	19.46	−0.19	−0.97
	P2-2	21.15	22.01	0.86	4.06
	P2-3	23.31	22.06	−1.25	−5.34
P3	P3-1	13.75	17.76	4.00	29.11
	P3-2	14.68	17.90	3.22	21.92
	P3-3	13.86	22.49	8.63	62.23

**Table 5.** Experimental validation for non-Darcy permeability and flow index

Mixture	Sample	Experiment		Simulation		Percent error in $k$	Percent error in $m$
		Non-Darcy permeability coefficient, $k$ (mm/s)	Flow index, $m$	Non-Darcy permeability coefficient, $k$ (mm/s)	Flow index, $m$		
P1	P1-1	15.53	0.461	15.83	0.529	1.95	14.67
	P1-2	16.23	0.478	16.48	0.529	1.51	10.68
	P1-3	13.48	0.450	13.79	0.526	2.34	16.99
P2	P2-1	12.77	0.447	13.03	0.510	2.05	14.01
	P2-2	16.71	0.493	16.82	0.512	0.68	3.73
	P2-3	18.50	0.485	18.70	0.513	1.08	5.82
P3	P3-1	13.39	0.445	13.68	0.515	2.10	15.55
	P3-2	11.62	0.487	11.71	0.516	0.74	5.99
	P3-3	16.62	0.442	17.00	0.517	2.28	16.95

past fluid flow in porous media studies (Hutter et al. 2011; Pedras and de Lemos 2001; Della Torre et al. 2014), the characterization of fluid flow regimes was carried out using the following:

- Darcy flow regime ( $Re < 1$ ).
- Forchheimer flow regime ( $1 < Re < 150$ ).
- Post-Forchheimer flow regime ( $150 < Re < 300$ ).
- Fully turbulent flow ( $Re > 300$ ).

The mean effective pore diameter was determined by employing DIP algorithms, specifically the ungrouping and watershed segmentation algorithms. These algorithms play a crucial role in accurately assessing the pore network properties. Neglecting these algorithms, along with the thresholding algorithm, can lead to significant errors in pore network properties (Jagadeesh et al. 2019a, b, 2020) and Reynolds number calculations. Furthermore, it is important to highlight that using the average velocity (seepage velocity divided by effective porosity) (Zhang et al. 2018; Chen et al. 2018) instead of the seepage velocity (Tan et al. 1997; Bear 1972) can result in an overestimation of the Reynolds number and mischaracterization of the flow regime. Details on the DIP algorithms can be found in Jagadeesh et al. (2019a) and Ong et al. (2020).

### Validation of XRCT-Based Numerical Model

Tables 4 and 5 compare experimental and XRCT-based effective porosity, non-Darcy permeability, and flow index values. The following observations can be made:

- The percentage error for effective porosity lies in the range of  $-1\%$  to  $30\%$  (except for P3-3) and the non-Darcy permeability coefficient lies in the range of  $0\%$  to  $3\%$ . These errors are considerably lower compared with previous numerical studies (Masad et al. 2007; Zhang et al. 2018; Kutay et al. 2007; Yu et al. 2019; Chen et al. 2021; Fedele et al. 2020; Qian et al. 2020). This improvement can be attributed to the appropriate usage of DIP algorithms and the modeling of turbulent flows as highlighted in Jagadeesh et al. (2019a). In addition the error in the effective porosity values are attributed to the experimental errors using ASTM C1754-12 Drying Method B.
- The flow index values fall within the range of  $0.44$  to  $0.53$ , indicating a turbulent regime of fluid flow. These findings align with the results reported in previous experimental studies (Fwa et al. 1998; Hatanaka et al. 2019) and numerical studies (Jagadeesh et al. 2019a; Ong et al. 2020).

Overall, the comparison between experimental- and XRCT-based data highlights the relatively low errors in effective porosity and non-Darcy permeability coefficients. Moreover, the flow index values consistently indicate a turbulent flow regime, in accordance with previous research findings in both experimental and numerical

studies. It is clear that the developed XRCT-based model and DIP algorithms are capable of predicting the fluid flow characteristics and can be used to investigate the effect of varying hydraulic gradients on Darcy and non-Darcy permeability characteristics for different pervious concrete mixtures. The combination of XRCT data, finite-volume modeling, and CFD simulations provides a robust framework for analyzing the fluid flow behavior and predicting permeability properties of pervious concrete.

### Comparison of Laboratory and Field Permeability Using XRCT-Based Numerical Model

Fig. 4 shows the variation of the hydraulic gradient versus specific discharge results for Sample P1-1 along with Darcy, Forchheimer,

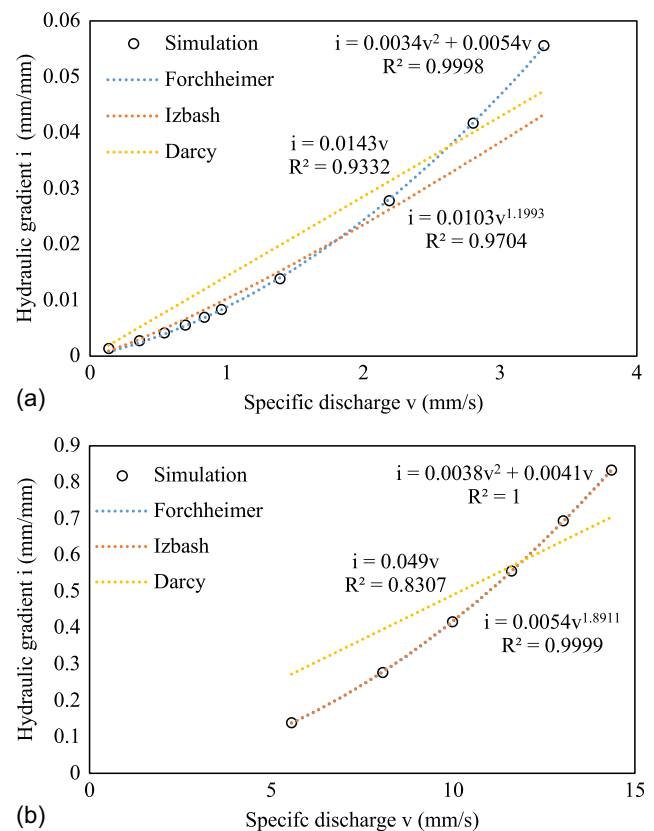


**Fig. 4.** Darcy, Forchheimer, and Izbash permeability parameters for Sample P1-1: (a) field hydraulic heads varying from 0.25 to 10 mm; and (b) laboratory hydraulic heads varying from 25 to 150 mm.

**Table 6.** Comparison of Darcy permeability coefficient at laboratory and field hydraulic heads

Mixture	Sample	Darcy permeability coefficient, $k$ (mm/s)		
		Laboratory head	Field head	Error (%)
P1	P1-1	19.73	67.50	-70.77
	P1-2	20.53	70.02	-70.68
	P1-3	17.22	59.31	-70.98
P2	P2-1	16.39	59.87	-72.62
	P2-2	21.14	77.52	-72.73
	P2-3	23.48	85.31	-72.48
P3	P3-1	17.16	62.03	-72.33
	P3-2	14.68	52.86	-72.22
	P3-3	21.32	76.59	-72.17

**Table 7.** Comparison of Izbash permeability coefficients at laboratory and field hydraulic heads

Mixture	Sample	Laboratory head		Field head		Error (%)	
		$k$ (mm/s)	$m$	$k$ (mm/s)	$m$	$k$ (mm/s)	$m$
P1	P1-1	15.83	0.529	45.55	0.834	-65.25	-36.58
	P1-2	16.48	0.529	45.45	0.825	-63.75	-35.88
	P1-3	13.79	0.526	37.31	0.815	-63.02	-35.47
P2	P2-1	13.03	0.510	29.23	0.744	-55.44	-31.44
	P2-2	16.82	0.512	38.44	0.747	-56.25	-31.54
	P2-3	18.70	0.513	44.22	0.760	-57.72	-32.44
P3	P3-1	13.68	0.515	32.27	0.760	-57.62	-32.28
	P3-2	11.71	0.516	29.37	0.777	-60.13	-33.57
	P3-3	17.00	0.517	41.63	0.772	-59.15	-32.98

and Izbash equations for different hydraulic head ranges. The range of hydraulic heads adopted in this paper is based on the values that are expected in the field (typically ranging from 0.25 to 150 mm). The following observations can be made from the figure:

- The Darcy equation does not fit the flow regime at different hydraulic head ranges [Figs. 4(a and b)] and this is in line with past experimental and numerical studies on nonlinearity in the fluid flow (Masad et al. 2007; Zhang et al. 2018; Hatanaka et al. 2019; Huang et al. 2010; Martin et al. 2014; West et al. 2016; Tan et al. 1999).
- Non-Darcy equations (Izbash and Forchheimer) fit the flow regimes well for different hydraulic head ranges. In addition to the preceding, Tables 6–8 compare the effect of hydraulic head on permeability parameters using Darcy, Izbash, and Forchheimer equations. It can be found from these tables that:
  - The use of laboratory hydraulic head results in significant underestimation of permeability parameters for Darcy (error up to -73%) and Izbash equations (error up to -66% for permeability coefficient and -37% for flow index) and overestimation for Forchheimer equations (error up to 148% for permeability coefficient and 14% for Forchheimer coefficient) compared with field hydraulic heads. This is in line with the findings by Fwa et al. (1998) where the effect of various laboratory hydraulic gradients on Izbash permeability was studied and the authors reported a difference of about 10% between the maximum and minimum permeability coefficients.
  - It can also be observed from Table 7 for laboratory and field flow index values that as the hydraulic head range increases, the average flow index  $m$  increases from 0.5 to 0.8 (laboratory

**Table 8.** Comparison of Forchheimer permeability coefficients at laboratory and field hydraulic heads

Mixture	Sample	Laboratory head		Field head		Error (%)	
		$k$ (mm/s)	$\beta$ (1/mm)	$k$ (mm/s)	$\beta$ (1/mm)	$k$ (mm/s)	$\beta$ (1/mm)
P1	P1-1	242.54	36,897.0	185.60	33,300.4	30.68	10.80
	P1-2	257.86	34,123.6	190.73	30,772.0	35.20	10.89
	P1-3	234.30	48,892.2	168.07	43,933.4	39.41	11.29
P2	P2-1	733.14	57,026.2	232.40	50,087.8	215.47	13.85
	P2-2	748.50	34,055.0	302.76	29,939.0	147.23	13.75
	P2-3	717.36	27,479.2	314.17	24,157.0	128.34	13.75
P3	P3-1	477.55	51,254.0	229.89	45,824.8	107.74	11.85
	P3-2	364.96	69,697.6	188.25	62,043.8	93.87	12.34
	P3-3	454.13	32,830.0	274.12	29,625.4	65.67	10.82

$m < \text{field } m$ ), indicating a transition regime at the field head and turbulent regime at the laboratory head.

In summary, comparing laboratory and field conditions highlights significant discrepancies in permeability parameters. Laboratory hydraulic heads result in underestimated permeability for Darcy and Izbash equations, while overestimation occurs with the Forchheimer equation. Moreover, the analysis of flow index values demonstrates a transition regime at field hydraulic heads and a turbulent regime at laboratory hydraulic heads, emphasizing the influence of hydraulic head range on flow behavior. Overall, the proper evaluation of permeability characteristics must be carried out at the field hydraulic gradients using non-Darcy permeability parameters.

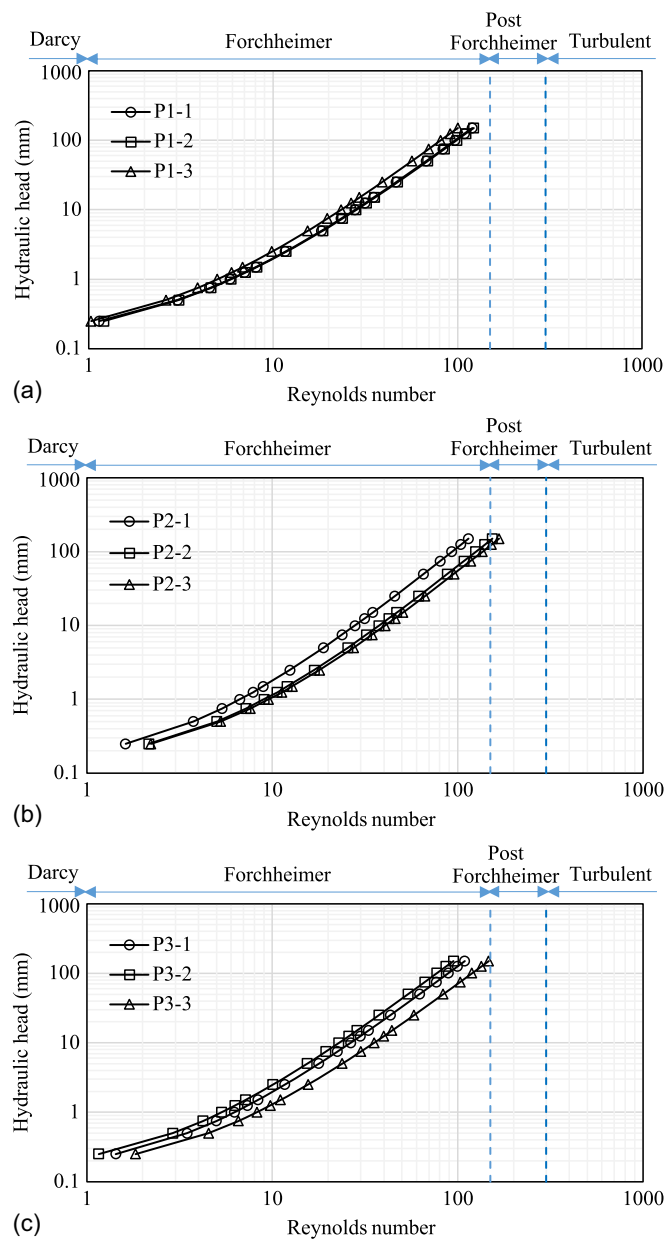
### Characterization of Fluid Flow Regime Using XRCT-Based Numerical Model

Fig. 5 shows the results of fluid flow regime characteristics at various hydraulic heads (ranging from 0.25 to 150 mm) and various samples. The following are the observations made:

- As the hydraulic head value reduces, the Reynolds number reduces, representing the change in flow regime for all pervious concrete samples.
- The Reynolds number for various samples lies in the range of 1 to 150, representing the Forchheimer flow regime as discussed in the section “Methodology,” except P2-2 and P2-3, which slightly exceed the Reynolds number of 150, representing the post-Forchheimer flow regime.
- This also proves that Darcy’s law ( $Re < 1$ ) does not exist at lower head values. This is unlike the findings reported by Zhang et al. (2018), Chen et al. (2018), and Wen et al. (2020), who reported the linear flow characteristics at field heads using Reynolds number with the lack of importance on DIP algorithms and velocities as discussed in Table 1.
- Comparing Samples P1 and P2, Sample P1 with the smaller aggregate sizes exhibits a lower Reynolds number compared with Sample P2 with the larger aggregate sizes. The P3 mixture exhibits the intermediate Reynolds number characteristics because of its intermediate aggregate gradation with respect to P1 and P2. Overall, it must be understood that the flow regime in pervious concrete mixtures exhibits the nonlinearity in the flow characteristics at both the laboratory and field hydraulic gradients.

### Conclusions

This study was aimed at investigating the research gap of the effect of laboratory and field hydraulic heads on various permeability



**Fig. 5.** Fluid flow regime characterization at various hydraulic heads: (a) Sample P1; (b) Sample P2; and (c) Sample P3.

parameters such as Darcy, Forchheimer, and Izbash parameters, and quantifying the flow regime characteristics of different pervious concrete mixtures at field hydraulic gradients through the use of XRCT-based numerical modeling. At first, the validation for the major pore network properties was carried out using laboratory experiments. The evaluation of permeability characteristics at laboratory and field hydraulic gradients for various pervious samples was carried out for different fluid flow equations. Finally, the characterization of fluid flow regime was carried out using accurate DIP algorithms. The following conclusions were drawn from this study:

- The existing permeability measurement setups in the laboratory do not replicate the actual field conditions (at lower hydraulic heads). This was found using the XRCT-based permeability simulation models in the current study.
- The use of laboratory hydraulic head results in significant underestimation of permeability parameters compared with the field

hydraulic heads for Darcy and Izbash equations, and overestimation for Forchheimer equations.

- Non-Darcy equations are well suited for the evaluation of pervious concrete fluid flow analyses at field hydraulic gradients.
- The fluid flow behavior in pervious concrete mixtures was found to be nonlinear and exhibits transition flow regime at both laboratory and field hydraulic gradients.

Although the developed XRCT-based model was effective in quantifying laboratory errors in permeability, it requires substantial computational resources and cost. In addition, the discharge-based thresholding algorithm used in conjunction with the model requires extensive calibration, resulting in time-consuming efforts. Nevertheless, the findings presented in this paper emphasize the importance of XRCT-based modeling in bridging the gap between laboratory and field permeabilities, thereby enhancing our understanding of the non-Darcy permeability of pervious pavements. This research can potentially assist engineers in designing effective drainage systems for full-scale pervious pavements. Future investigation should focus on exploring modeling across a larger variation in mix designs and also study the impact of laboratory and field hydraulic heads on various elements of pervious pavement drainage design.

## Data Availability Statement

Some or all data, models, or code that support the findings of this study are available from the corresponding author upon reasonable request.

## References

- ACI (American Concrete Institute). 2010. *Report on pervious concrete*. ACI 522R-2010. Farmington Hills, MI: ACI.
- ASTM. 2012. *Standard test method for density and void content of hardened pervious concrete*. ASTM C1754-12/C1754M. West Conshohocken, PA: ASTM.
- ASTM. 2016. *Standard specification for Portland cement*. ASTM C150-16E1. West Conshohocken, PA: ASTM.
- ASTM. 2017. *Standard test method for infiltration rate of in place pervious concrete*. ASTM C1701/C1701M-17a. West Conshohocken, PA: ASTM.
- Bear, J. 1972. *Dynamics of fluids in porous media*. New York: American Elsevier.
- BSI (British Standards Institution). 2012. *Bituminous mixtures. Test methods for hot mix asphalt. Permeability of specimen*. BS EN 12697-19:2012. London: BSI.
- Chandrupa, A. K., and K. P. Biligiri. 2016. "Comprehensive investigation of permeability characteristics of pervious concrete: A hydrodynamic approach." *Constr. Build. Mater.* 123 (Jun): 627–637. <https://doi.org/10.1016/j.conbuildmat.2016.07.035>.
- Chen, J., X. Yin, H. Wang, X. Ma, Y. Ding, and G. Liao. 2018. "Directional distribution of three-dimensional connected voids in porous asphalt mixture and flow simulation of permeability anisotropy." *Int. J. Pavement Eng.* 21 (12): 1–13. <https://doi.org/10.1080/10298436.2018.1555330>.
- Chen, S., Z. You, S. L. Yang, A. Garcia, and L. Rose. 2021. "Influence of air void structures on the coefficient of permeability of asphalt mixtures." *Powder Technol.* 377 (Jan): 1–9. <https://doi.org/10.1016/j.powtec.2020.08.082>.
- Chen, X., H. Wang, C. Li, W. Zhang, and G. Xu. 2020. "Computational investigation on surface water distribution and permeability of porous asphalt pavement." *Int. J. Pavement Eng.* 23 (4): 1–13. <https://doi.org/10.1080/10298436.2020.1797734>.
- Cooley, L. A., Jr. 1999. *Permeability of Superpave mixtures: Evaluation of field permeameters*. NCAT Rep. No. 99-1. Auburn, AL: National Center for Asphalt Technology.
- Della Torre, A., G. Montenegro, G. R. Tabor, and M. L. Wears. 2014. "CFD characterization of flow regimes inside open cell foam substrates."

- Int. J. Heat Fluid Flow* 50 (Apr): 72–82. <https://doi.org/10.1016/j.ijheatfluidflow.2014.05.005>.
- Fedele, V., N. Berloco, P. Colonna, A. Hertrich, P. Intini, V. Ranieri, and J. J. Sansalone. 2020. “Computational fluid dynamics as a tool to estimate hydraulic conductivity of permeable asphalts.” *Transp. Res. Rec.* 2674 (8): 370–383. <https://doi.org/10.1177/0361198120927390>.
- Fwa, T., S. Tan, and C. Chuai. 1998. “Permeability measurement of base materials using falling-head test apparatus.” *Transp. Res. Rec.* 1615 (1): 94–99. <https://doi.org/10.3141/1615-13>.
- Fwa, T. F., S. A. Tan, and Y. K. Guwe. 2001. “Rational basis for evaluation and design of pavement drainage layers.” *Transp. Res. Rec.* 1772 (1): 174–180. <https://doi.org/10.3141/1772-21>.
- Gruber, I., I. Zinovik, L. Holzer, A. Flisch, and L. D. Poulikakos. 2012. “A computational study of the effect of structural anisotropy of porous asphalt on hydraulic conductivity.” *Constr. Build. Mater.* 36 (Aug): 66–77. <https://doi.org/10.1016/j.conbuildmat.2012.04.094>.
- Hatanaka, S., Z. Kamalova, and M. Harada. 2019. “Construction of a non-linear permeability model of pervious concrete and drainage simulation of heavy rain in a residential area.” *Results Mater.* 3 (Oct): 100033. <https://doi.org/10.1016/j.rinma.2019.100033>.
- Huang, B., H. Wu, X. Shu, and E. G. Burdette. 2010. “Laboratory evaluation of permeability and strength of polymer-modified pervious concrete.” *Constr. Build. Mater.* 24 (5): 818–823. <https://doi.org/10.1016/j.conbuildmat.2009.10.025>.
- Hutter, C., A. Zenklusen, S. Kuhn, and P. R. von Rohr. 2011. “Large eddy simulation of flow through a streamwise-periodic structure.” *Chem. Eng. Sci.* 66 (3): 519–529. <https://doi.org/10.1016/j.ces.2010.11.015>.
- Jagadeesh, A., G. P. Ong, and Y. M. Su. 2020. “Effect of global thresholding algorithms on pervious concrete pore network properties using XRCT-based digital image processing.” In *Proc., 9th Int. Conf. on Maintenance and Rehabilitation of Pavements—Mairepav9*, 575–585. Berlin: Springer.
- Jagadeesh, A., G. P. Ong, and Y.-M. Su. 2019a. “Development of discharge-based thresholding algorithm for pervious concrete pavement mixtures.” *J. Mater. Civ. Eng.* 31 (9): 04019179. [https://doi.org/10.1061/\(ASCE\)MT.1943-5533.0002807](https://doi.org/10.1061/(ASCE)MT.1943-5533.0002807).
- Jagadeesh, A., G. P. Ong, and Y.-M. Su. 2019b. “Evaluation of pervious concrete pore network properties using watershed segmentation approach.” In *Proc., Airfield and Highway Pavements 2019: Testing and Characterization of Pavement Materials*, 437–446. Reston, VA: ASCE.
- Kutay, M. E., A. H. Aydilek, E. Masad, and T. Harman. 2007. “Computational and experimental evaluation of hydraulic conductivity anisotropy in hot-mix asphalt.” *Int. J. Pavement Eng.* 8 (1): 29–43. <https://doi.org/10.1080/10298430600819147>.
- Martin, W. D., III, N. B. Kaye, and B. J. Putman. 2014. “Impact of vertical porosity distribution on the permeability of pervious concrete.” *Constr. Build. Mater.* 59 (Jun): 78–84. <https://doi.org/10.1016/j.conbuildmat.2014.02.034>.
- Masad, E., A. Al Omari, and H. C. Chen. 2007. “Computations of permeability tensor coefficients and anisotropy of asphalt concrete based on microstructure simulation of fluid flow.” *Comput. Mater. Sci.* 40 (4): 449–459. <https://doi.org/10.1016/j.commatsci.2007.01.015>.
- Ong, G. P., A. Jagadeesh, and Y. M. Su. 2020. “Effect of pore network characteristics on non-Darcy permeability of pervious concrete mixture.” *Constr. Build. Mater.* 259 (Oct): 119859. <https://doi.org/10.1016/j.conbuildmat.2020.119859>.
- Pedras, M. H., and M. J. de Lemos. 2001. “Macroscopic turbulence modeling for incompressible flow through undeformable porous media.” *Int. J. Heat Mass Transfer* 44 (6): 1081–1093. [https://doi.org/10.1016/S0017-9310\(00\)00202-7](https://doi.org/10.1016/S0017-9310(00)00202-7).
- Qian, N., D. Wang, D. Li, and L. Shi. 2020. “Three-dimensional mesoscopic permeability of porous asphalt mixture.” *Constr. Build. Mater.* 236 (Mar): 117430. <https://doi.org/10.1016/j.conbuildmat.2019.117430>.
- Tan, S. A., T. F. Fwa, and K. C. Chai. 2004. “Drainage considerations for porous asphalt surface course design.” *Transp. Res. Rec.* 1868 (1): 142–149. <https://doi.org/10.3141/1868-15>.
- Tan, S. A., T. F. Fwa, and C. T. Chuai. 1997. “A new apparatus for measuring the drainage properties of porous asphalt mixes.” *J. Test. Eval.* 25 (4): 370–377. <https://doi.org/10.1520/JTE11872J>.
- Tan, S. A., T. F. Fwa, and C. T. Chuai. 1999. “Automatic field permeameter for drainage properties of porous asphalt mixes.” *J. Test. Eval.* 27 (1): 57–62. <https://doi.org/10.1520/JTE12160J>.
- Tan, S. A., T. F. Fwa, and V. Y. Guwe. 2000. “Laboratory measurements and analysis of clogging mechanism of porous asphalt mixes.” *J. Test. Eval.* 28 (3): 207–216. <https://doi.org/10.1520/JTE12096J>.
- Wen, F., H. Fan, S. Zhai, K. Zhang, and F. Liu. 2020. “Pore characteristics analysis and numerical seepage simulation of antifreeze permeable concrete.” *Constr. Build. Mater.* 255 (Jun): 119310. <https://doi.org/10.1016/j.conbuildmat.2020.119310>.
- West, D., N. B. Kaye, B. J. Putman, and R. Clark. 2016. “Quantifying the non-linear hydraulic behavior of pervious concrete.” *J. Test. Eval.* 44 (6): 20150054. <https://doi.org/10.1520/JTE20150054>.
- Young, P. G., T. B. H. Beresford-West, S. R. L. Coward, B. Notarberardino, B. Walker, and A. Abdul-Aziz. 2008. “An efficient approach to converting three-dimensional image data into highly accurate computational models.” *Philos. Trans. R. Soc. London A: Math. Phys. Eng. Sci.* 366 (1878): 3155–3173. <https://doi.org/10.1098/rsta.2008.0090>.
- Yu, F., D. Sun, M. Hu, and J. Wang. 2019. “Study on the pores characteristics and permeability simulation of pervious concrete based on 2D/3D CT images.” *Constr. Build. Mater.* 200 (Mar): 687–702. <https://doi.org/10.1016/j.conbuildmat.2018.12.135>.
- Zhang, J., G. Ma, R. Ming, X. Cui, L. Li, and H. Xu. 2018. “Numerical study on seepage flow in pervious concrete based on 3D CT imaging.” *Constr. Build. Mater.* 161 (Feb): 468–478. <https://doi.org/10.1016/j.conbuildmat.2017.11.149>.